Invariance of optimal composite waveguide geometries with respect to permittivity of the metal cladding

Joseph S. T. Smalley,* Matthew W. Puckett, and Yeshaiahu Fainman

Department of Electrical and Computer Engineering, University of California, San Diego, 9500 Gilman Drive, La Jolla, California 92023, USA

**Corresponding author: jsmalley@ucsd.edu*

Received September 5, 2013; revised September 30, 2013; accepted November 2, 2013; posted November 6, 2013 (Doc. ID 197169); published November 27, 2013

We optimize the threshold gain for cylindrical composite (semiconductor–dielectric–metal) waveguides (WGs) with various metal claddings. We show that the optimal dielectric width is invariant with respect to the imaginary part of the permittivity of the metal, ε''_M, and weakly dependent on the real part, ε'_M. To explain this behavior, we compare optimal geometries of WGs with different semiconductor permittivities, ε'_G. Results from these comparisons indicate that the optimal effective index parallels the optimal threshold gain in its relation to ε_M. We use our results to heuristically propose an analytical expression for the optimal threshold gain that approximates the numerical solution to within a factor of two over the range of explored ε'_G. Finally, we use data from our optimizations to obtain approximate analytical expressions for the optimal dielectric width and threshold gain as functions of the total WG radius.

OCIS codes: (310.4165) Multilayer design; (310.6628) Subwavelength structures, nanostructures; (000.4430) Numerical approximation and analysis; (260.3910) Metal optics; (140.5960) Semiconductor lasers; (230.7370) Waveguides.

http://dx.doi.org/10.1364/OL.38.005161

Since their inception a half-decade ago [1], subwavelength metal-clad lasers have become the subject of intense research. Because the cladding prevents coupling among devices, such nanolasers make particularly strong candidates for densely packed arrays of individually addressable coherent sources [2]. Recent demonstrations of continuous-wave operation via electrical injection near and at room temperature [3,4] suggest that subwavelength metal-clad lasers may become practical elements of such nanophotonic arrays. Metals, however, are lossy at telecom wavelengths, and this shortcoming necessitates the incorporation of dielectric shields into nanolaser designs.

Mizrahi *et al.* [5] first introduced the shield, a low refractive index dielectric layer located between the gain region and metal cladding, which mitigates the losses incurred from the overlap of the electromagnetic mode with the metal. Employing the equivalence between a circularly symmetric infinite waveguide (WG) and a cylindrical laser cavity with perfectly reflecting end mirrors, Mizrahi *et al.* used a numerical technique to show that a nonobvious optimal shield width exists for a composite (semiconductor–dielectric–metal) WG (CWG) with a fixed total radius. The optimal shield reduces the metal loss without displacing too much of the gain medium and corresponds to the shield width that yields the minimum threshold gain. To date, researchers have reported a number of lasers, both optically and electrically driven, designed with an optimized shield to reduce the threshold of the lasing "photonic" mode [3–4,6–8]. Research has also progressed in metallic lasers supporting plasmonic modes [9,10]. While the results of this Letter do apply to such devices, we have found that the introduction of the shield to the structure of Ref. [10], for example, only increases the threshold gain of the lasing mode. Therefore, the results of this Letter hold the most significance for devices utilizing photonic modes.

The choice of metal cladding affects laser design, fabrication, and performance in several ways. Perhaps most obviously, different metals exhibit varying degrees of loss or, equivalently, the imaginary part of the electric permittivity, ε''_M, differs for each metal. Additionally, metals adhere differently to the shield layer (usually SiO_2 or SiN [3–8]), react differently with etchants, and exhibit differing stability to the ambient environment. Thus, the ability to predict the behavior of a given CWG structure for a wide range of possible metal claddings holds significant value.

Recent experimental work [4] has suggested that the true optimal shield width ought to account for both thermal and electromagnetic effects. When thermal effects are considered, the shield width should be reduced because the thermal resistance of the low-index dielectric usually exceeds that of any other material in the structure. As a result, the true optimal shield width will be less than that suggested by a model that accounts for electromagnetic effects only. The optimal shield width obtained from the method of Ref. [5], therefore, may be considered as an upper bound to the true optimum.

Consider the cylindrical CWG with material and geometrical properties, as well as refractive index and electric field profiles, described by Fig. 1. The semiconductor core, lossless dielectric shield, and metal cladding are characterized electrically with permittivities $\varepsilon_G = \varepsilon'_G + j\varepsilon''_G$, ε_D, and $\varepsilon_M = \varepsilon'_M - j\varepsilon''_M$, respectively. The width of the shield layer Δ_D is given by the difference $\Delta_D = R_{\text{total}} - R_{\text{core}}$. In general, the electromagnetic field inside such a CWG may be expressed as an infinite, discrete sum of solutions to the source-free wave equation, the natural modes of the CWG. Assuming the CWG consists of nonmagnetic materials, each mode may be described by its complex wavenumber k, defined as $k^2 = \varepsilon_R k_0^2 = \varepsilon_R \omega^2/c^2 = \varepsilon_R(2\pi/\lambda_0)^2 = \beta_\rho^2 + \beta_z^2$ where, generally, the relative permittivity, ε_R, and the transverse and longitudinal propagation constants, β_ρ and β_z, respectively, are all complex [11], and λ_0 is the free space wavelength. Along with ε_R, β_ρ differs within each layer of the CWG, whereas β_z remains constant everywhere for a

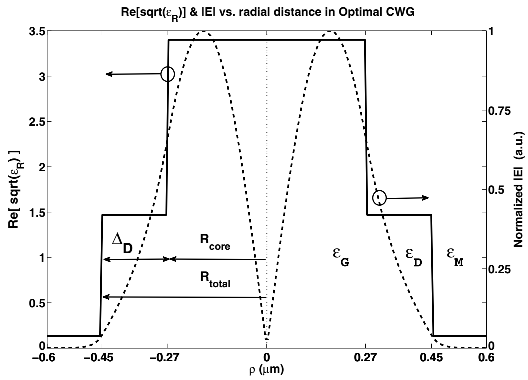

Fig. 1. Re(sqrt(ε_R)) and $|\boldsymbol{E}|$ of the TE_{01} mode as functions of radial distance in an optimized composite WG (CWG) at $\lambda_0 = 1.55$ μm. The permittivities are $\varepsilon_G = 11.56 + j8.65e-4$, $\varepsilon_D = 2.16$, and $\varepsilon_M = -130 - j3.0$, respectively.

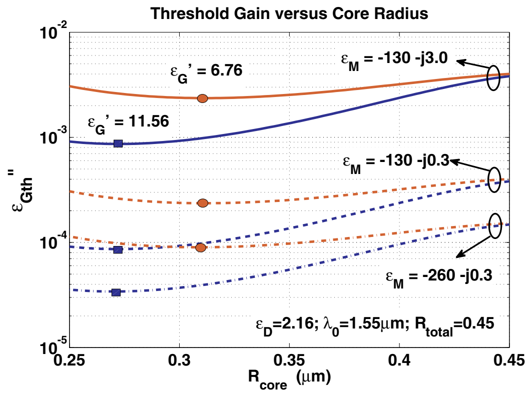

Fig. 2. Threshold gain ε''_{Gth} as function of R_{core} for two values of ε'_G, with ε_M parameterized. Blue rectangles and red circles indicate $(R_{core}, \varepsilon''_G) = (R_{core,opt}, \varepsilon_{Gth,opt}'')$ for InGaAsP and GaS CWGs, respectively. ε_D, λ_0, and R_{total} are fixed at 2.16, 1.55, and 0.45 μm, respectively.

given mode [11]. The boundary value problem to be solved consists of finding the eigenvalues to the system of transcendental equations that describes the CWG. In this Letter, we work under the threshold condition, $\beta''_z = 0$, and the eigenvalues correspond to the zeros in the complex $(\varepsilon''_G, \beta'_z)$ plane. Further, we concern ourselves only with the TE_{01} mode because this mode exhibits more favorable properties for use in a nanolaser than neighboring modes [5].

The threshold gain, ε''_{Gth}, is the value of ε''_G necessary to offset the metal loss and make the imaginary part of the propagation constant vanish; i.e., $\varepsilon''_{Gth} = \varepsilon''_G(\beta''_z = 0)$ [5]. It is related to the material threshold gain per unit length, g_{th}, via $g_{th} = 2\pi\varepsilon''_{gth}/(\lambda_0 n_g)$, where n_g is the group refractive index [12]. It is obvious that, all else equal, a more lossy metal will lead to a larger threshold gain. However, what is not immediately clear is the effect of the metal loss on the optimal shield width. Intuitively it seems that, all else equal, a CWG with a high-loss metal, such as aluminum at room temperature, $|\varepsilon''_M| \gg 1$, necessitates a thicker optimal shield for the TE_{01} mode than a low-loss metal, such as silver or aluminum at a lower temperature, $|\varepsilon''_M| \sim 1$. However, our intuition is wrong. The optimal shield width increases discontinuously, from zero when $\varepsilon''_M = 0$, to a constant, nonobvious value for all $\varepsilon''_M > 0$.

Applying the methodology of Ref. [5] to the material-geometry system in Fig. 1 with fixed R_{total}, and varying only ε_M, we observe that the optimal shield width, $\Delta_{D,opt}$, or, equivalently, the optimal core radius, $R_{core,opt}$, is constant with respect to changes in ε''_M and nearly constant with ε'_M. These results are shown in Fig. 2, where ε''_{Gth} is plotted as a function of R_{core} with ε_M and ε'_G as parameters. Constants include $\varepsilon_D = 2.16$, $\lambda_0 = 1.55$ μm, and $R_{total} = 0.45$ μm. The chosen value of R_{total} is sufficiently large to yield relatively low ε''_{Gth}, but also sufficiently small to yield a relatively high spontaneous emission factor, for a laser cavity based on this CWG. The parameterized metal permittivities are $-130 - j3.0$ (bold line), $-130 - j0.3$ (dash line), and $-260 - j0.3$ (dashed–dotted line), approximately representative of silver at room temperature, silver at liquid nitrogen temperature, and aluminum at liquid helium temperature, all near $\lambda_0 = 1.55$ μm, respectively [13–15]. The two values of ε'_G are 11.56 (blue) and 6.76 (red), representative of InGaAsP and GaS, respectively [16]. With the order of magnitude reduction in ε''_M, $R_{core,opt}$ of the InGaAsP (GaS) CWG remains constant at 0.272 μm (0.313 μm), and changes by less than 1% (2%), with the doubling of $|\varepsilon'_M|$. Equivalently, $\Delta_{D,opt}$ remains constant with ε''_M and varies from 0.178 to 0.180 μm (0.137 to 0.141 μm) with $|\varepsilon'_M|$. Consistent with the reasoning that a less lossy metal requires less compensation from the gain medium, we further observe that an order of magnitude change in ε''_M causes an order of magnitude reduction in ε''_{Gth} for both CWGs. Finally, we see that as $|\varepsilon'_M|$ is increased by a factor of two, ε''_{Gth} decreases by a factor of 2.53 (2.63).

Accompanying the invariance of $R_{core,opt}$ with respect to ε''_M and its weak dependence on ε'_M, the real part of the optimal effective index, $n_{eff,opt}'$, where $n_{eff} = \beta_z(2\pi/\lambda_0)$ and $n_{eff,opt} = n_{eff}(R_{core,opt})$, similarly exhibits invariance and weak dependence upon ε''_M and ε'_M, respectively. In Fig. 3, we show that $n_{eff,opt}'$ remains constant as ε''_M is reduced by an order of magnitude. When $|\varepsilon'_M|$ is doubled, $n_{eff,opt}'$ changes by less than 1% (2%), for the InGaAsP (GaS) CWGs. When considering a larger range of ε'_G values, as shown in Fig. 4, we observe that both $\Delta_{D,opt}$ and $n_{eff,opt}$ increase monotonically with ε'_G.

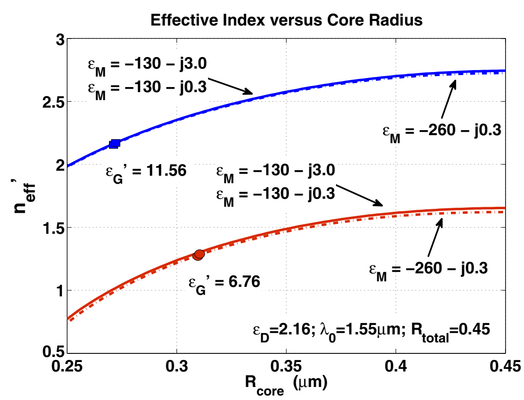

Fig. 3. n'_{eff} as function of R_{core} for two values of ε'_G, with ε_M parameterized. Blue rectangles and red circles indicate $(R_{core}, n_{eff}) = (R_{core,opt}, n_{eff,opt})$ for InGaAsP and GaS CWGs, respectively. ε_D, λ_0, and R_{total} are fixed at 2.16, 1.55, and 0.45 μm, respectively.

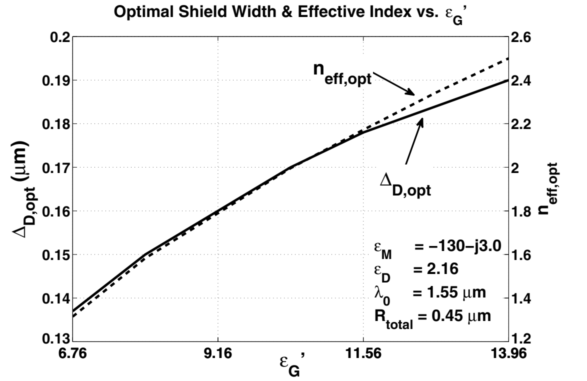

Fig. 4. $\Delta_{D,\text{opt}}$ and $n_{\text{eff,opt}}$ as functions of ε_G'. ε_M, ε_D, λ_0, and R_{total} are fixed at, $-130 - j3.0$, 2.16, 1.55, and 0.45 μm, respectively.

Inspection of the explicit definition of threshold gain [5] helps to explain the observed behavior in terms of the electric field $\boldsymbol{E}$,

$$\varepsilon_{G\text{th}}'' = \frac{\varepsilon_M'' \int_{\text{Metal}} |\boldsymbol{E}|^2 \mathrm{d}A}{\int_{\text{Gain}} |\boldsymbol{E}|^2 \mathrm{d}A} = \frac{\varepsilon_M'' \int_{R_{\text{total}}}^{\infty} |\boldsymbol{E}(\rho)|^2 \rho \mathrm{d}\rho}{\int_0^{R_{\text{core}}} |\boldsymbol{E}(\rho)|^2 \rho \mathrm{d}\rho}, \qquad (1)$$

where the second equality is introduced for modes with azimuthal symmetry, such as the TE_{01} mode under consideration. Allowing ourselves the heuristic assumption that the electric field inside a bulk polarized material with relative permittivity, ε_R, is reduced from its free space value by a factor of ε_R [11], then, according to Eq. (1), we would anticipate that $\varepsilon_{G\text{th}}''$ is proportional to $\varepsilon_M''(\varepsilon_G')^2/(\varepsilon_M')^2$. However, Fig. 2 shows that $\varepsilon_{G\text{th}}''$ increases with a decreasing ε_G'. Obviously, our problem does not consist of a bulk-polarized medium, so we modify our heuristic approach by incorporating n_{eff} into the proportionality. Namely, by studying the results of Fig. 4, we observe that $\varepsilon_{G\text{th}}''$ is roughly proportional to $\varepsilon_G'^2$, if we reduce ε_G' by the factor n_{eff}^2 to account for the guided nature of the mode inside the CWG. Hence, we posit an approximate expression to Eq. (1),

$$\varepsilon_{G\text{th,opt}}'' \cong \varepsilon_M''\{\varepsilon_G'/[\varepsilon_M'(n_{\text{eff}}^{\text{opt}})^2]\}^2. \qquad (2)$$

In Fig. 5, we plot $\varepsilon_{G\text{th,opt}}''$ according to Eq. (2) as a function of ε_G', along with the numerical solution to Eq. (1). We observe that Eq. (2) approximates the numerical solution to within a factor of two for all ε_G'. Furthermore, if $\varepsilon_{G\text{th}}''$ and n_{eff} are substituted for $\varepsilon_{G\text{th,opt}}''$ and $n_{\text{eff,opt}}$, then Eq. (2) approximates the numerical solution to Eq. (1) within a factor of two for all $R_{\text{core}} > 300$ nm. Figure 6 shows the percentage error in Eq. (2), with this substitution over the range of R_{core} and ε_G' values used in Figs. 3–5. The error is defined as $100|\varepsilon_{G\text{th},N}'' - \varepsilon_{G\text{th},A}''|/\varepsilon_{G\text{th},N}'$, where the subscripts N and A refer to numerical and analytical, respectively. We observe that in the region of most interest to the designer, i.e., near $R_{\text{core,opt}}$, the error is quite low, while it increases rapidly for smaller R_{core}, due to the more rapid variation of n_{eff} with decreasing R_{core}, per Fig. 3. Admittedly, Eq. (2) is not rigorously derived; however, it clearly holds value as a design tool.

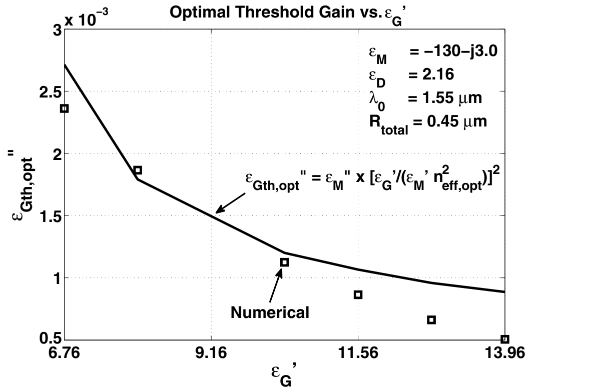

Fig. 5. $\varepsilon_{G\text{th,opt}}''$ as function of ε_G', (open squares) numerical solutions of Eq. (1) and (solid line) analytical approximation of Eq. (2). ε_M, ε_D, λ_0, and R_{total} are fixed at $-130 - j3.0$, 2.16, 1.55, and 0.45 μm, respectively.

We summarize the nonintuitive main result of this Letter in the following manner. We begin with a material-geometry selection and solve the original eigenvalue problem by obtaining the zeros in the $(\varepsilon_G'', \beta_z')$ plane [5]. We continue this process, varying R_{core} with R_{total} fixed, until a minimum threshold gain, $\varepsilon_{G\text{th,opt}}''$, and the corresponding $R_{\text{core,opt}}$ and $n_{\text{eff,opt}}$ are found. Next, we change the metal permittivity. The zeros in the $(\varepsilon_G'', \beta_z')$ plane necessarily shift. However, by maintaining the imposed threshold condition, $n_{\text{eff}}'' = 2\pi\beta_z''/\lambda_0 = 0$, we force ε_G'' to respond proportionally to changes in ε_M''. Because n_{eff}' remains unchanged or changes very slightly, the electric field distribution in the CWG remains unchanged or changes very slightly. Prior to changing ε_M, the electric field distribution was such that $\varepsilon_{G\text{th}}'' = \varepsilon_{G\text{th,opt}}''$, and so it follows that the new threshold gain is also an optimum. The virtual lack of change of n_{eff}' and the constraint that $n_{\text{eff}}'' = 0$ are sufficient conditions for the invariance and weak dependence of $\Delta_{D,\text{opt}}$ (equivalently, $R_{\text{core,opt}}$) with respect to ε_M'' and ε_M', respectively.

The invariance and weak dependence of $\Delta_{D,\text{opt}}$ on ε_M'' and ε_M' implies that, once an optimized geometry is found for a given set of ε_G', ε_D, and λ_0, different metals may be used without affecting the numerical results. For example, if laser cavities employing silver cladding are

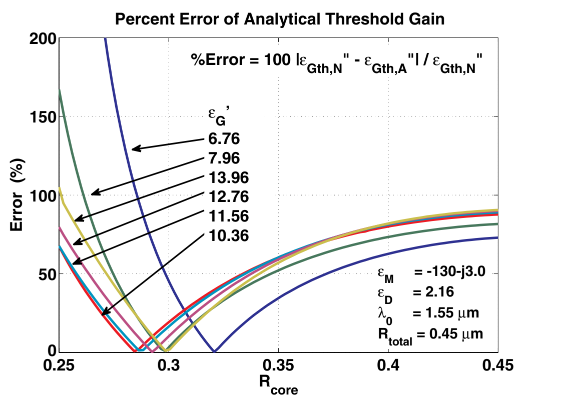

Fig. 6. Error in Eq. (2), with $\varepsilon_{G\text{th}}''$ and n_{eff} substituted for $\varepsilon_{G\text{th,opt}}''$ and $n_{\text{eff,opt}}$, relative to the numerical solution of Eq. (1) as a function of R_{core} with ε_G' parameterized. ε_D, ε_M, λ_0, and R_{total} are fixed at 2.16, $-130 - j3.0$, 1.55, and 0.45 μm, respectively.

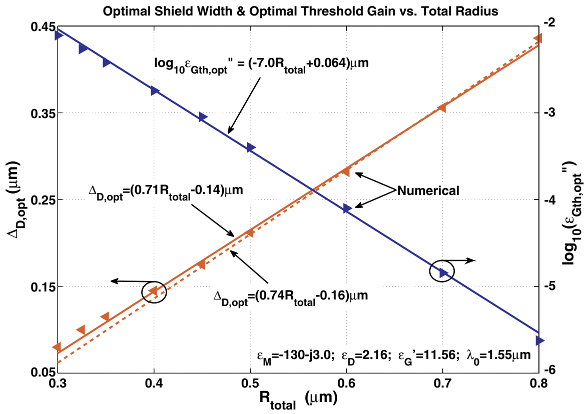

Fig. 7. $\Delta_{D,\text{opt}}$ and $\log_{10}(\varepsilon_{G\text{th,opt}}'')$ as functions of R_{total}. The red (on red line from lower left to upper right) and blue (on blue line from upper left to lower right) solid triangles correspond to numerical solutions of Eq. (1), whereas the red and blue lines correspond to linear approximations for $\Delta_{D,\text{opt}}$ and $\log_{10}(\varepsilon_{G\text{th,opt}}'')$, respectively. ε_M, ε_D, ε_G', and λ_0 are fixed at $-130 - j3.0$, 2.16, 11.56, and 1.55 μm, respectively.

rigorously designed, they need not be redesigned if the fabrication process necessitates the use of gold or aluminum claddings. Furthermore, data obtained from executing the optimization procedure over a wide geometric parameter space may be used in the development of approximate analytical expressions to expedite the design process. Based on the preceding results, approximations to $\Delta_{D,\text{opt}}$ may be applied to structures with an arbitrary metal cladding. We present several analytical approximations that we have discovered through the use of our numerical optimization scheme. All of the results were verified for material properties representative of the InGaAsP CWG at $\lambda_0 = 1.55$ μm.

The optimal shield thickness $\Delta_{D,\text{opt}}$ is nearly a linear function of R_{total}, as seen in Fig. 7. An approximation to the numerical solution that describes this relation is $\Delta_{D,\text{opt}} \sim (0.71R_{\text{total}} - 0.14)$ μm, which is accurate to within 2.5% over the range of R_{total} values from 0.30 to 0.70 μm. For the range of R_{total} values above 0.45 μm, a better fit is $\Delta_{D,\text{opt}} \sim (0.74R_{\text{total}} - 0.16)$ μm, which is accurate to within 1%.

While the value of $\varepsilon_{G\text{th,opt}}''$ does depend upon ε_M'', we may still approximate it in a similar fashion. In Fig. 7 we also plot the numerical solution of $\log_{10}(\varepsilon_{G\text{th,opt}}'')$ versus R_{total} on a linear scale. Clearly, the logarithm of $\varepsilon_{G\text{th,opt}}''$ is almost inversely proportional to R_{total}. An approximation expressing this fact, $\log_{10}(\varepsilon_{G\text{th,opt}}'') = (-7R_{\text{total}} + 0.064)$ μm, is also plotted, and is accurate to within 10% over the range of R_{total} values from 0.35 to 0.75 μm. Thus, we may approximate $\varepsilon_{G\text{th,opt}}''$ explicitly in terms of the material parameters via Eq. (2), or implicitly through the total radius via a logarithmic approximation.

In conclusion, we have used a numerical technique [5] for threshold gain optimization of CWGs and, implicitly, laser cavities. We have shown that $\Delta_{D,\text{opt}}$ is invariant with respect to ε_M'' and weakly dependent upon ε_M', and explained this via the corresponding behavior of n_{eff}'. We have further shown that $\varepsilon_{G\text{th,opt}}''$ may be approximated by $\varepsilon_M''(\varepsilon_G')^2/(\varepsilon_M'(n_{\text{eff,opt}}')^2)$. Finally, we have formulated several analytical approximations useful for the expedited design of optimally functioning semiconductor–dielectric–metal nanolaser cavities.

The authors would like to thank Dr. Boris Slutsky for helpful discussions. This work was supported by DARPA, the NSF, through the Center for Integrated Access Networks (CIAN) ERC, the Cymer Corporation, the Army Research Office, and the Office of Naval Research MURI.

References

1. M. T. Hill, Y. Oei, B. Smalbrugge, Y. Zhu, T. de Vries, P. J. van Veldhoven, F. W. M. van Otten, T. J. Eijkemans, J. P. Turkiewicz, H. de Waardt, E. J. Geluk, S. Kwon, Y. Lee, R. Notzel, and M. K. Smit, Nat. Photonics **1**, 589 (2007).
2. Q. Gu, J. S. T. Smalley, M. P. Nezhad, A. Simic, J. H. Lee, M. Katz, O. Bondarenko, B. Slutsky, A. Mizrahi, V. Lomakin, and Y. Fainman, "Sub-wavelength semiconductor lasers for dense chip-scale integration," Adv. Photonics Res., submitted for publication
3. J. H. Lee, M. Khajavikhan, A. Simic, Q. Gu, O. Bondarenko, B. Slutsky, M. P. Nezhad, and Y. Fainman, Opt. Express **19**, 21524 (2011).
4. K. Ding, M. T. Hill, Z. C. Liu, P. J. van Veldhoven, and C. Z. Ning, Opt. Express **21**, 4728 (2013).
5. A. Mizrahi, V. Lomakin, B. A. Slutsky, M. P. Nezhad, L. Feng, and Y. Fainman, Opt. Lett. **33**, 1261 (2008).
6. M. Nezhad, A. Simic, O. Bondarenko, B. Slutsky, A. Mizrahi, L. Feng, V. Lomakin, and Y. Fainman, Nat. Photonics **4**, 395 (2010).
7. Q. Ding, A. Mizrahi, Y. Fainman, and V. Lomakin, Opt. Lett. **36**, 1812 (2011).
8. K. Ding, L. Yin, M. T. Hill, Z. Liu, P. J. van Veldhoven, and C. Z. Ning, Appl. Phys. Lett. **102**, 041110 (2013).
9. R. F. Oulton, V. J. Sorger, T. Zentgraf, R. Ma, C. Gladden, L. Dai, G. Bartal, and X. Zhang, Nature **461**, 629 (2009).
10. M. Khajavikhan, A. Simic, M. Katz, J. H. Lee, B. Slutsky, A. Mizrahi, V. Lomakin, and Y. Fainman, Nature **482**, 204 (2012).
11. H. A. Auda and D. Kajfez, in *Dielectric Resonators*, D. Kajfez and P. Guillon, eds., (Artech House, 1986).
12. A. Saleh and J. Dionne, Phys. Rev. B **85**, 045407 (2012).
13. P. B. Johnson and R. W. Christy, Phys. Rev. B **6**, 4370 (1972).
14. A. D. Rakic, Appl. Opt. **34**, 4755 (1995).
15. J. McKay and J. A. Rayne, Phys. Rev. B **13**, 673 (1976).
16. K. Kato and N. Umemura, Opt. Lett. **36**, 746 (2011).